Bioorganic Chemistry 37 (2009) 6–10

Contents lists available at ScienceDirect

Bioorganic Chemistry

journal homepage: www.elsevier.com/locate/bioorg

Effects of petrosaspongiolide R on the surface topology of bee venom PLA_2: A limited proteolysis and mass spectrometry analysis

Maria Chiara Monti, Raffaele Riccio, Agostino Casapullo *

Dipartimento di Scienze Farmaceutiche, Università degli Studi di Salerno, Via Ponte don Melillo, 84084 Fisciano, Italy

ARTICLE INFO

Article history:
Received 8 July 2008
Available online 21 October 2008

Keywords:
Phospholipase A_2
Marine natural inhibitor
Surface topology
Limited proteolysis
Mass spectrometry

ABSTRACT

Petrosaspongiolides are sponge metabolites belonging to the family of the γ-hydroxybutenolide marine terpenoids. They possess a remarkable *in vitro* and *in vivo* anti-inflammatory profile, due to the specific inhibition of group II and III secretory phospholipase A_2 enzymes, and for this reason can be considered as potential lead for the development of anti-inflammatory drugs. The molecular mechanism of bee venom phospholipase A_2 inactivation has been identified, and the ligand–enzyme complex formation is guided by either non-covalent and covalent interactions. In this work we have analyzed the conformational changes induced by petrosaspongiolide R on the bee venom phospholipase A_2 topology during the molecular recognition process, through the application of limited proteolysis and mass spectrometric methodologies. The results are indicative of structural changes at the N- and C-terminal domains producing a more compact conformational arrangement of the enzyme.

1. Introduction

A number of marine metabolites are known to possess anti-inflammatory activity [1–4]. Petrosaspongiolides M-R (PM-PR) are marine sesterterpenes structurally characterized by a γ-hydroxybutenolide moiety. They have shown an *in vitro* and *in vivo* potent anti-inflammatory activity, mediated by specific inhibition of secretory phospholipase A_2 (*s*PLA_2 enzymes), such as bee venom (*bv*PLA_2), *Naja naja* and human synovial phospholipase A_2 preparations, suggesting a remarkable wide therapeutic spectrum for these marine metabolites in inflammatory diseases [5–9]. In this context, *bv*PLA_2 represents a very useful enzymatic model, since an excellent correlation between the inhibition of PM-PR has been obtained on *bv*PLA_2 with respect to human secretory counterpart [5,6]. The molecular mechanism underlying the sub-micromolar irreversible inhibition of the bee venom PLA_2 (*bv*PLA_2) by PM has been clarified combining mass spectrometry (MS) and molecular modeling approaches. The N-terminal amino group (Ile-1 residue), recently identified as the unique PM covalent binding site on this enzyme, selectively delivers a nucleophilic attack onto the masked aldehyde at C-25 of the pharmacophoric γ-hydroxybutenolide ring of PM, giving rise to a Schiff base [10–12].

Moreover, a comparative analysis on the whole petrosaspongiolide family allowed a better comprehension of the molecular recognition processes regulating the inhibitor–enzyme interaction [11,12]. A full characterization of the *bv*PLA_2 adduct with PR, one of the least active and most structurally different among petrosaspongiolides, by LC–MS, MS^n, and computational methods, confirmed the same inhibition mechanism and covalent binding site already found for PM. Finally, extensive molecular docking studies performed in comparison on the PM-PLA_2 and PR-PLA_2 complexes provided critical insight on how the balance between non-covalent and covalent inhibitor–enzyme interactions may affect the final potency exhibited by the various compounds of the petrosaspongiolide family [11]. In our interpretation of the data, the correct arrangement of the ligand in the active site, induced by non-covalent interactions, is of pivotal importance in the inactivation process, and also responsible for the high covalent bonding ability of PM in respect of the very low one of PR [11].

Analysis of the structure of PR and PM complexes with the *bv*PLA_2 have revealed many details of the interactions occurring during the molecular recognition process, even if a number of peculiar features of the topological changes occurring in the whole enzyme structure remain to be fully clarified.

The aim of this paper is to shed more lights on the conformational changes induced on *bv*PLA_2 topology upon the complex formation with petrosaspongiolides, that could be helpful for a future rational design of appropriate inhibitors.

This investigation has been performed by combining limited proteolysis with mass spectrometric methodologies, a procedure developed to explore the surface topology of proteins and the interface regions in protein complexes [13–17]. We selected PR as the best probe among petrosaspongiolides for this investigation, due to its reactivity profile and the peculiar experimental procedure. Indeed, PR is the unique among petrosaspongiolides able to

* Corresponding author. Fax: +39 089 969602.
E-mail address: casapullo@unisa.it (A. Casapullo).

0045-2068/$ - see front matter © 2008 Elsevier Inc. All rights reserved.
doi:10.1016/j.bioorg.2008.09.001

generate the solely monomodified *bv*PLA_2-ligand species, after enzyme incubation and chemical reduction of the Schiff base with $NaBH_4$ [11]. The reductive treatment of the complex, giving rise to an amine function, is essential to preserve the complex during the following purification, disulfide reduction and proteolysis steps.

The conformational changes taking place within the *bv*PLA_2 tertiary structure under the influence of its inhibitor PR, confirmed by CD measures, have been analyzed under different physico-chemical conditions. The results are suggestive of evident structural changes, mainly affecting the N- and C-terminal domains, producing a more compact conformational arrangement of the enzyme.

2. Materials and methods

2.1. Limited proteolysis experiments on the isolated *bv*PLA_2

bvPLA_2 protein was provided by Sigma–Aldrich Co. An aliquot of a *bv*PLA_2 protein (50 μM in $Na_2B_4O_7{\cdot}10H_2O$ 10 mM a pH 7.4) was diluted with an appropriate volume of the enzyme-containing solution in order to obtain the selected enzyme:substrate ratio (w:w). The final concentration of *bv*PLA_2 was fixed at 25 μM. The mixture was incubated at 25 °C and the enzymatic reaction was monitored collecting aliquots of 100 μl after 15, 30 and 60 min of incubation. The proteolytic activity was blocked adding 5 μl of 20% TFA and freezing each aliquots by liquid nitrogen. Trypsin, chimotrypsin, endoproteases GluC and LysC were chosen as proteolytic agents using an enzyme:substrate ratio from 1:250 and 1:1000 (w:w).

Sample aliquots were loaded on a C4 *narrow-bore* (250 × 2 mm, 300 °A Jupiter, Phenomenex) on an Agilent HP1000 instrument using a linear gradient from 25% to 95% of acetonitrile–water with 0.1% of TFA over 45 min. The elution profile was monitored at 220 and 280 nm and the collected fraction were analyzed by ESI-MS on a LCQ-Deca (ThermoFinnigan).

Because of the presence of five disulfide bridges which prevent the release of all the peptides obtained from the *bv*PLA_2 proteolysis, it was necessary to reduce the sample. The protein fraction obtained from HPLC was diluted in a denaturing buffer (Guanidine Chloride 6 M, Tris–aminomethane 0.1 M, EDTA 1 mM, pH 7.5) containing DTT 2.5 mM and kept under argon for 2 h at 37 °C. The peptide separation was achieved by RP-HPLC on a C-18 *narrow-bore* column (250 × 2 mm 300 °A Jupiter, Phenomenex) by means of a linear gradient from 15% to 95% of acetonitrile–water with 0.1% of TFA over 60 min. Chromatographic peaks were collected and analyzed by ESI-MS and tandem ESI-MS.

2.2. Circular dichroism experiments

Circular dichroism measurements were performed by using a Jasco J-810 spectrometer equipped with a cell holder thermostatically controlled by a circulating water bath. Measurements were recorded at 25 °C, with a 8-s time constant, and at a rate of 5 nm/min and were averaged for 8 acquisitions. The spectra of the protein (25 μM) were collected with rectangular quartz cells of 1-cm path length in the near-UV region (320–250 nm) and of 1-mm path length in the far-UV region (250–190 nm). The free *bv*PLA_2 and the *bv*PLA_2–PR complex, after purification on a PD-10 column, were analyzed before and after the treatment with $NaBH_4$ (molar excess of 400:1, kept for 2 h in ice) in sodium borate buffer (10 mM, pH 7.5). All spectra were routinely corrected for the background signal and for dilution effects. Additionally, the spectra of *bv*PLA_2–PR complex were subtracted to that of PR.

2.3. Limited proteolysis experiments on the *bv*PLA_2–PR complex

bvPLA_2 (10 nmol) were incubated in presence of petrosaspongiolide R (molar excess of fivefold) in a final volume of 250 μl in sodium borate buffer 10 mM a pH 7.4 for 10 min at 40 °C. PR was diluted in isopropanol at final concentration of 5 mM in order to add only few μl of organic solvent to the *bv*PLA_2 sample to prevent protein unfolding. A molar excess of 400 times of $NaBH_4$ was added to the mixture in a volume of 300 μl of NaOH 15 mM aqueous solution without any pH change and the reaction was kept in ice for 2 h. To remove the excess of free PR, the sample was loaded on a PD-10 column (Pharmacia) and gently eluted with NaB_4O_7 buffer at neutral pH. The fraction were manually collected, analyzed by UV spectrophotometer at 220 and 280 nm, and lyophilized. Moreover, RP-HPLC-MS analysis were carried out to confirm the presence of the protein complex and the absence of free PR. A C4 *narrow-bore* (250 × 2 mm 300 °A Jupiter, Phenomenex) with a linear gradient from 25% to 95% of acetonitrile–water with 0.1% of TFA over 45 min was used. The sample was diluted again in sodium borate 10 mM at neutral pH up to a 50 μM concentration as determined by BioRad assay. The limited proteolysis procedure was identical to the one described above. The optimal enzyme:substrate ratio was 1:50 (w:w).

3. Results and discussion

The influence of PR on the *bv*PLA_2 conformational arrangement during the inhibition process was firstly monitored by measuring CD spectra of the free protein and its complex with PR, and then analyzed by limited proteolysis and mass spectrometry approach, comparing the different peptide maps obtained from the protein in absence and in presence of its inhibitor. *bv*PLA_2–PR complex formation was assessed by mass spectrometry measurements (Fig. 1).

3.1. CD experiments

Samples of the free and PR bound *bv*PLA_2 were separately analyzed by CD both in the far and the near-UV regions, to assess the changes induced by the inhibitor in the secondary and/or tertiary structure of the protein [18–20]. CD spectra of *bv*PLA_2 with PR were collected after 10 min incubation at 40 °C. The measurement was re-

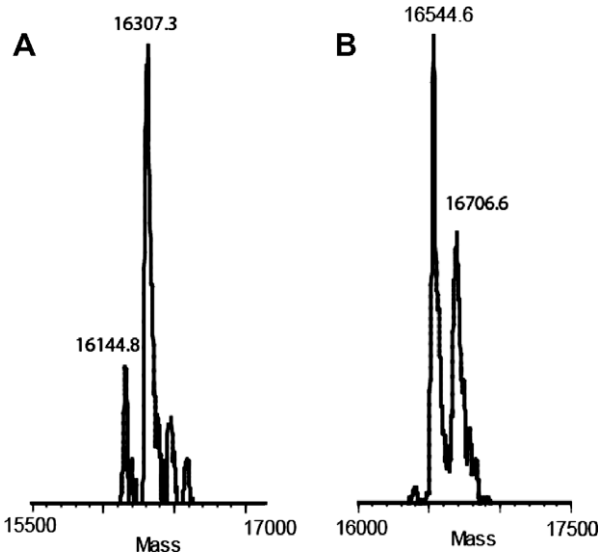

Fig. 1. Deconvoluted MS spectra of the most abundant glycoforms of *bv*PLA_2 (A) and *bv*PLA_2–PR complex (B). ΔM_W is 399.8 Da, in agreement with the covalent modification of the enzyme previously reported [11].

peated after reduction of *bv*PLA$_2$–PR complex with $NaBH_4$ in a molar excess of 400:1 for 120 min in ice and purification on a PD-10 column, giving rise to the same results. The CD curves recorded in the far-UV region (250–190 nm) concerning the isolated *bv*PLA$_2$ and its PR complex were perfectly superimposable, suggesting that PR did not interfere with the protein secondary structure (data not shown).

On the contrary, different curves were obtained in the region between 250 and 320 nm, where the CD effect arises from the aromatic side chains, namely two Trp, eight Tyr and five Phe residues in the case of *bv*PLA$_2$. The contribution of the aromatic side chains onto the near-UV-CD spectra of proteins is widely recognized and utilized as a sensitive probe of protein conformation. The differences observed in the CD spectra (at 250–320 nm) of the free and PR-bound enzyme were clearly indicative of a perturbation of the enzyme environment induced by the inhibitor (Fig. 2).

3.2. Topological studies of *bv*PLA$_2$ (limited proteolysis experiments)

The surface topology of *bv*PLA$_2$ was probed by a combined approach that integrates limited proteolysis and mass spectrometric procedures. Limited proteolysis experiments were performed using trypsin, chymotrypsin, endoproteinase GluC and LysC as proteolytic probes, according to the strategy previously described [12,13].

Native *bv*PLA$_2$ was incubated with each protease using an appropriate enzyme-to-substrate ratio, and the extent of enzymatic hydrolysis was monitored on a time-course basis by sampling the incubation mixture at different times (15, 30, 60 min) followed by RP-HPLC fractionation. The occurrence of five disulfide bridges in the tertiary structure of *bv*PLA$_2$ (Cys9–Cys31; Cys30–Cys70; Cys37–Cys63, Cys61–Cys95, Cys105–Cys113) prevented the release of free peptide fragments after the enzymatic cleavage, leading to the formation of a single partially hydrolyzed protein species. Therefore, the chromatographic fraction containing the latter species together with the intact protein was lyophilized, dissolved in a denaturing buffer and then submitted to disulfide bridges reduction with DTT (see Section 2 for details). The following release of the peptide fragments was monitored by RP-HPLC and the identification of the peptides by ESI-MS led to the assignment of the cleavage sites on the *bv*PLA$_2$.

As an example, Fig. 3A shows the RP-HPLC chromatograms of the aliquots withdrawn following 15 and 60 min of endoproteinase GluC digestion (see Table 1 for further details). Protein *bv*PLA$_2$ was cleaved at Glu110, as resulted from the fragments 1–110 and 111–134 monitored into the HPLC trace above the peak 3 and 2, respectively. After 60 min of enzyme incubation, a secondary cleavage site was detected at the level of Glu 20, as indicated by the appearance of the peak 1 (fragment 1–20). Moreover, in the chromatogram were also monitored peak 2 and 3, the last containing three different species

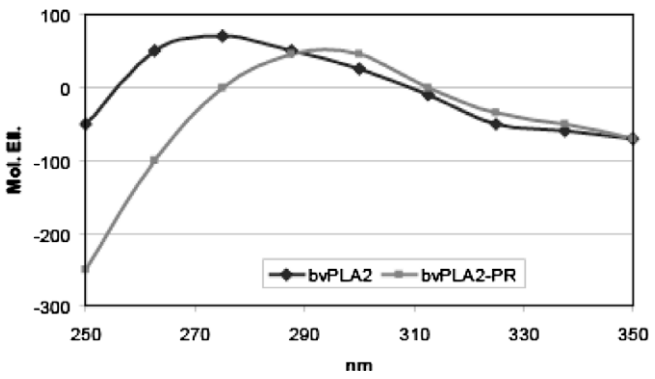

Fig. 2. CD curves of free *bv*PLA$_2$ and *bv*PLA$_2$–PR complex.

at molecular weight of 13134.5 Da (fragment 21–134), 13127.6 Da (fragment 1–110) and 16155.5 Da (intact and reduced *bv*PLA$_2$). The overall data from the limited proteolysis experiments on the isolated *bv*PLA$_2$ are summarized in Table 1 and Fig. 4.

Preferential cleavage sites were classified as "primary" and "secondary," merely on qualitative kinetic evaluation, according to their rate of appearance and accumulation during the time-course experiments.

The primary cleavage sites on the *bv*PLA$_2$ surface are located within the C-terminal segment 110–112, indicating that this region is particulary flexible and exposed to the protease action. Moreover, the N-terminal area from amino acid 14–24 is also prone to the enzymatic cleavage even if with a slower kinetic profile. Our gathered data indicate a considerable conformational flexibility of these two regions on the protein surface corresponding to unstructured loops.

3.3. Topological studies of *bv*PLA$_2$–PR complex (limited proteolysis experiments)

The conformational changes occurring within the *bv*PLA$_2$ structure upon PR influence were finely investigated by a comparative analysis, employing the same limited proteolysis-mass spectrometry approach previously described.

A sample of *bv*PLA$_2$ was firstly incubated with PR for 10 min at 40 °C, and then $NaBH_4$ was added in a molar excess of 400:1 for 120 min in ice. The reaction mixture was then loaded on a PD-10 column for gently separate the protein fraction from the unreacted PR. The fraction containing the unreacted *bv*PLA$_2$ and *bv*PLA$_2$–PR species was lyophilized and diluted in NaB_4O_7 buffer 10 mM at pH 7.4 up to a concentration of 50 μM and subsequently submitted to limited proteolysis experiments. After proteolysis at 25 °C for 15, 30 and 60 min the aliquots were fractionated by RP-HPLC. The fraction containing the intact and partially hydrolyzed *bv*PLA$_2$–PR complex was purified and submitted to disulfide bridges reduction with DTT (as reported above), giving rise to the free fragmented peptides and the identification of the cleavage sites on the *bv*PLA$_2$–PR adduct.

The overall data from the limited proteolysis experiments on the *bv*PLA$_2$–PR complex are summarized in Table 2 and Fig. 4. When these data were compared with those obtained on the isolated protein (Table 1 and Fig. 3B), a number of considerations could be drawn. The complex showed a lower accessibility to proteases than the isolated protein, as demonstrated by the higher E/S ratio (1:50) required to observe proteolytic cleavages, thus suggesting that the interaction with PR led to a further increase in the compactness of the *bv*PLA$_2$ structure.

As an example, Fig. 3B shows the HPLC chromatograms of the complex aliquots digested by endoprotease GluC after 15 and 60 min of incubation. LC–MS analysis clearly indicates Glu 20 as unique proteolytic cleavage site on the protein, generating the 21–134 and the glycosilated 1–20 peptides (M_W of 3022.9 and 13134.5 Da, respectively).

The whole results indicate that the main conformational changes occurred within the C-terminal tail, a region less flexible and exposed than in the free protein, due to a nearly complete protection of 110–112 amino acid residues. The accessibility of N-terminal region was also strongly decreased by PR as a logical consequence of the conformational changes following the covalent binding of the inhibitor to the Ile1.

4. Discussion

Differences in the *bv*PLA$_2$ conformational arrangement in the presence of its inhibitor petrosaspongiolide R were monitored by

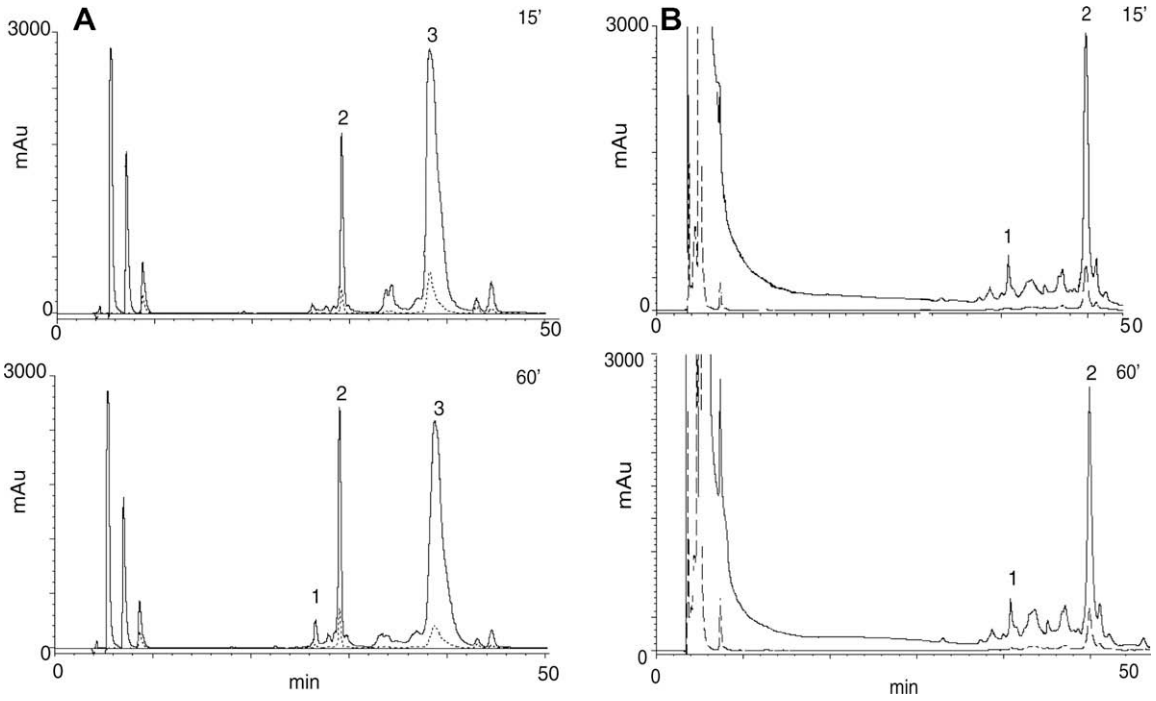

Fig. 3. HPLC analysis (λ of 220 and 280 nm) of *bv*PLA$_2$ (A) and *bv*PLA$_2$–PR complex (B) digested with endoprotease GluC under controlled conditions at 15 and 60 min of hydrolysis using enzyme:substrate ratio of 1:1000 w:w on *bv*PLA$_2$ (A) and 1:50 w:w on *bv*PLA$_2$–PR complex (B). Individual fractions were collected and analyzed by ESI-MS. (A) Fraction 1 contained the peptide 1–20 glycosilated, fraction 2 contained the peptide 111–134 and fraction 3 contained the undigested *bv*PLA$_2$, together with the peptides 1–110 and 21–134. (B) Fraction 1 contained the peptide 21–134. Fraction 2 contained the undigested *bv*PLA$_2$–PR and the peptide 1–20 glycosylated bound to PR.

Table 1
Preferential cleavage sites detected on the isolated *bv*PLA$_2$[a]

Protease	Enzyme/substrate ratio	Primary sites	Secondary sites	M_W of peptides (Da)
Trypsin	1/500	Arg 112	Arg 23	1–23 = 3349.5, 24–134 = 12806.7, 1–112 = 13337.9, 113–134 = 2818.4
Endoproteinase Lys C	1/500	Lys 14	Lys 25	1–14 = 2451.4, 15–134 = 13705.6, 1–25 = 3624.5, 26–134 = 12532.8
Endoproteinase Glu C	1/1000	Glu 110	Glu 20	1–20 = 3022.9, 21–134 = 13134.5, 1–110 = 13127.6, 111–134 = 3031.2
Chymotrypsin	1/250	Phe 24		1–24 = 3496.5, 25–134 = 12660.0

[a] Different sites were classified merely on qualitative kinetic evaluation as primary (15 min proteolysis) and secondary (60 min proteolysis).

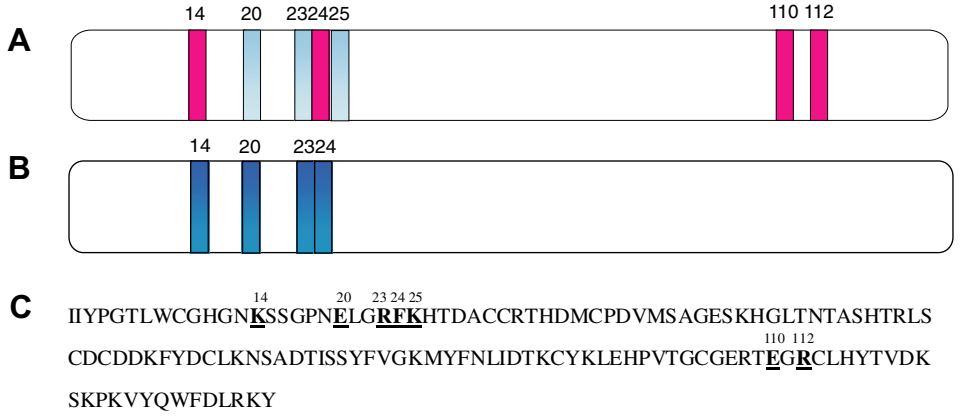

Fig. 4. Schematic summary of limited proteolysis experiments carried out on the free *bv*PLA$_2$ (A) and *bv*PLA$_2$–PR complex (B). Preferential cleavage sites are highlighted in pink for the free protein and in blue for the protein–ligand complex. Light blue bars indicated the secondary cleavage sites. (C) reports the cleavage sites on the *bv*PLA$_2$ sequence. (For interpretation of the references to color in this figure legend, the reader is referred to the web version of this article.)

CD and probed by limited proteolysis combined with mass spectrometric methodologies. The overall strategy is based on the evidence that amino acid residues located within exposed and flexible regions of a protein can be recognized by proteases, leading to a peculiar peptide map in accordance with the protein active conformation. Because the surface topology of the protein is affected by conformational changes during the complex formation with the inhibitor, a differential peptide map is obtained, from which protein regions involved in the structural changes could be inferred.

Table 2
Preferential cleavage sites detected on the *bv*PLA$_2$–PR complex[a]

Protease	Enzyme/substrate ratio	Primary sites	Secondary sites	M_W of peptides (Da)
Trypsin	1/50	Arg 23	/	1–23 = 3349.5, 24–134 = 12806.7
Endoproteinase Lys C	1/50	Lys 14	/	1–14 = 2451.4, 15–134 = 13705.6
Endoproteinase Glu C	1/50	Glu 20	/	1–20 = 3022.9, 21–134 = 13134.5
Chymotrypsin	1/50	Phe 24	/	1–24 = 3496.5, 25–134 = 12660.0

[a] Different sites were classified merely on qualitative kinetic evaluation as primary (15 min proteolysis) and secondary (60 min proteolysis).

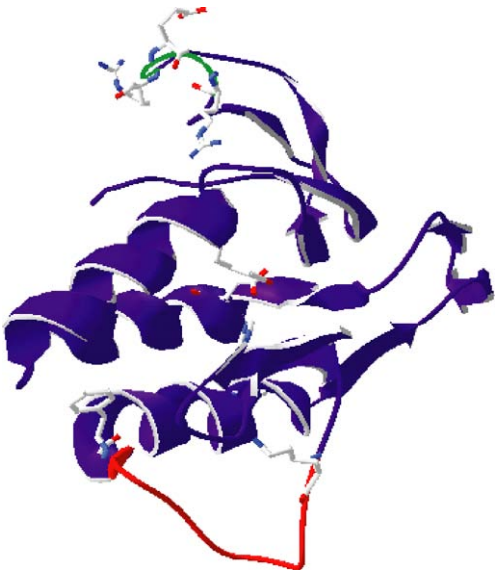

Fig. 5. Three-dimensional structure of *bv*PLA$_2$ (PDB code: 1POC). The backbone is in dark blue; preferential cleavage sites on the isolated *bv*PLA$_2$ are highlighted in red whereas in green are reported the preferential cleavage sites for the *bv*PLA$_2$–PR complex. The side chains of catalytic amino acids are visible in the active pocket in between the three α-helix. (For interpretation of the references to color in this figure legend, the reader is referred to the web version of this article.)

As first stage, we performed a CD comparative analysis between the free and PR bound *bv*PLA$_2$. Differences in the CD curves were evident only in the near-UV region (320–250 nm), suggesting that the interaction between the protein and PR produced a sensitive perturbation of the enzyme environment, without affecting the protein secondary structure.

On the basis of these results, we started to analyze the surface topology of the free *bv*PLA$_2$. This enzyme showed a compact structure with a low accessibility and a characteristic pattern of exposed and buried regions. The C-terminal segment encompassing the residues 108–112 was the most accessible portion where the preferential proteolytic cleavages were located, whereas other protease-sensitive sites were localized onto the 20–25 region at the N-terminal segment. Limited proteolysis data were essentially consistent with the crystal structure of the *bv*PLA$_2$, where the major accessibility of the C-terminal and N-terminal regions is due to their localization in an area located away from the protein core and endowed with high conformational flexibility (Fig. 5).

The structural changes occurring under the influence of the binding with PR revealed that the *bv*PLA$_2$–PR complex was more resistant than the free protein to proteolytic cleavages, as demonstrated by the E/S ratio increasing in the limited proteolysis experiments (Tables 1 and 2). Besides, the prevalence of enzymatic cleavage sites was located at the N-terminal 20–25 region, even if characterized by a lower reactivity than the free *bv*PLA$_2$ towards all the proteases. This result may be a direct consequence of an enhanced compactness of the N-terminal segment, due to the covalent modification of the Ile-1 residue by PR [11,12] and the following lower accessibility of the proteases onto the 20–25 residues. Further and major conformational changes were detected in the C-terminal region of *bv*PLA$_2$. As a matter of fact, the 108–112 region was strongly shielded from the proteolytic attack, as monitored in the HPLC traces and summarized in Table 2, as a consequence of a more compact and rigid conformational arrangement.

In conclusion, our data suggested that petrosaspongiolide R induces a dual effect on *bv*PLA$_2$ topology: it affects the N-terminal loop, located between the first β-strand and the α-helix-rich core of the protein (Fig. 5), as a consequence of the Ile-1 covalent modification, furthermore generating a *long range* effect in the C-terminal area which becomes more protected towards the protease activity.

Acknowledgments

Financial support by the University of Salerno is gratefully acknowledged. The authors also acknowledge the Centre of Competence in Diagnostics and Molecular Pharmaceutics for the use of their instruments, and Dr. C. Santomauro for her enthusiastic contribution.

References

[1] L. Gomez-Paloma, M.C. Monti, S. Terracciano, A. Casapullo, R. Riccio, Curr. Org. Chem. 9 (2005) 1419–1427.
[2] S. Terracciano, M. Rodriguez, M. Aquino, M.C. Monti, A. Casapullo, R. Riccio, L. Gomez-Paloma, Curr. Med. Chem. 13 (2005) 1947–1969.
[3] M.J. Alcaraz, M. Payá, Curr. Opin. Invest. Drugs 7 (2006) 974–979.
[4] R.A. Keyzers, M.T. Davies-Coleman, Chem. Soc. Rev. 24 (2005) 355–365.
[5] A. Randazzo, C. Debitus, L. Minale, P. Garcìa-Pastor, M.J. Alcazar, M. Payà, L. Gomez-Paloma, J. Nat. Prod. 61 (1998) 571–575.
[6] P. Garcìa-Pastor, A. Randazzo, L. Gomez-Paloma, M.J. Alcazar, M. Payà, J. Pharmacol. Exp. Ther. 289 (1999) 166–172.
[7] I. Posadas, M.C. Terencio, A. Randazzo, L. Gomez-Paloma, M.J. Alcazar, M. Payà, Biochem. Pharmacol. 65 (2003) 887–895.
[8] J. Busserolles, M. Payá, M.V. D'Auria, L. Gomez-Paloma, M.J. Alcaraz, Biochem. Pharmacol. 15 (2005) 1433–1440.
[9] A. Capasso, A. Casapullo, A. Randazzo, L. Gomez-Paloma, Life Sci. 73 (2003) 611–616.
[10] F. Dal Piaz, A. Casapullo, A. Randazzo, R. Riccio, P. Pucci, G. Marino, L. Gomez-Paloma, ChemBioChem 3 (2002) 664–671.
[11] M.C. Monti, A. Casapullo, R. Riccio, L. Gomez-Paloma, Bioorg. Med. Chem. 12 (2004) 1467–1472.
[12] M.C. Monti, A. Casapullo, R. Riccio, L. Gomez-Paloma, FEBS Lett. 578 (2004) 269–274.
[13] A. Fontana, P.P. de Laureto, B. Spolaore, E. Frare, P. Picotti, M. Zambonin, Acta Biochim. Pol. 51 (2004) 299–321.
[14] S.J. Hubbard, Biochim. Biophys. Acta 15 (1998) 191–206.
[15] P.P. de Laureto, L. Tosatto, E. Frare, O. Marin, V.N. Uversky, A. Fontana, Biochemistry 45 (2006) 11523–11531.
[16] A. Casbarra, L. Birolo, G. Infusini, F. Dal Piaz, M. Svensson, P. Pucci, C. Svanborg, G. Marino, Protein Sci. 13 (2004) 1322–1330.
[17] E. Bianchi, S. Orrù, F. Dal Piaz, R. Ingenito, A. Casbarra, G. Biasiol, U. Koch, P. Pucci, A. Pessi, Biochemistry 38 (1999) 13844–13852.
[18] S.M. Kelly, T.J. Jess, N.C. Price, Biochim. Biophys. Acta 1751 (2005) 119–139.
[19] B.M. Bulheller, A. Rodger, J.D. Hirst, Phys. Chem. Chem. Phys. 17 (2007) 2020–2035.
[20] N.J. Greenfield, Methods Enzymol. 383 (2004) 282–317.